Published in final edited form as:

Structure. 2003 May ; 11(5): 509–520.

Structure of the Predominant Protein Arginine Methyltransferase PRMT1 and Analysis of Its Binding to Substrate Peptides

Xing Zhang and **Xiaodong Cheng***

Department of Biochemistry, Emory University School of Medicine, 1510 Clifton Road, Atlanta, Georgia 30322

Summary

PRMT1 is the predominant type I protein arginine methyltransferase in mammals and highly conserved among all eukaryotes. It is essential for early postim-plantation development in mouse. Here we describe the crystal structure of rat PRMT1 in complex with the reaction product AdoHcy and a 19 residue substrate peptide containing three arginines. The results reveal a two-domain structure—an AdoMet binding domain and a barrel-like domain—with the active site pocket located between the two domains. Mutagenesis studies confirmed that two active site glutamates are essential for enzymatic activity, and that dimerization of PRMT1 is essential for AdoMet binding. Three peptide binding channels are identified: two are between the two domains, and the third is on the surface perpendicular to the strands forming the β barrel.

Keywords

protein arginine methylation; AdoMet-dependent methylation; glycine- and arginine-rich (GAR) sequence; RGG repeats; PRMT dimerization and oligomerization

Introduction

Protein arginine methylation is a common posttranslational modification in eukaryotes. The major type of *p*rotein arginine (*R*) *m*ethyl*t*ransferase (PRMT), type I, transfers the methyl group from S-adenosyl-L-methionine (AdoMet) to the guanidino group of arginines in protein substrates, resulting in monomethylarginine and asymmetric dimethylarginine in substrate proteins [1]. The best known substrates for type I PRMT are RNA binding proteins involved in various aspects of RNA processing and/or transport, such as hnRNPs, fibrillarin, nucleolin [2], and poly(A) binding protein II [3]. More recently, a growing number of other proteins have been found to be substrates of PRMT1, including high molecular weight fibroblast growth factor 2 (HMW FGF-2, a nuclear growth factor [4]), interleukin enhancer binding factor 3 (ILF3) [5], STAT1, a transcription factor activated by extracellular signals [6], and histone H4 [7, 8]. Most PRMT1 substrates contain *g*lycine- and *a*rginine-*r*ich

*Correspondence: xcheng@emory.edu.

Accession Numbers

The coordinates of the three PRMT1 structures have been deposited in the Protein Data Bank under ID codes 1ORI (pXC248), 1OR8 (pXC249), and 1ORH (pXC252), respectively.

(GAR) sequences that include multiple arginines in RGG or RXR contexts [2–4]. However, increasing numbers of substrates lacking GAR domain are being discovered [9], including STAT1 and histone H4, which contain no other arginines near the methylation target.

PRMT genes are present in eukaryotes from fungi to plants and animals. Though *Saccharomyces cerevisiae* has only one PRMT homolog [10, 11], multiple genes have been found in plants and animals. For example, six very similar paralogous mammalian PRMT genes have been reported so far: PRMT1, PRMT2, PRMT3, CARM1/PRMT4 [12–17], JBP1/PRMT5 [18, 19], and PRMT6 [20]. At least eight PRMTs are present in the completed *Drosophila melanogaster* genome (X.Z., unpublished observation). The presence of a large number of PRMTs may signify the diverse roles PRMTs can play.

How does arginine methylation affect protein function? There is some evidence that arginine methylation can affect a protein's affinity for RNA [21]. However, at least in the case of Hrp1p binding to its specific, high-affinity RNA target, arginine methylation does not seem to affect the strength of nucleic acid binding [22, 23]. More recent evidence suggests that arginine methylation affects the interaction of the substrate proteins with other proteins [6, 24, 25] as well as their subcellular localization in yeast and mammalian cells [26–29]. Arginine methylation has been implicated in receptor-mediated signaling [5, 12, 17, 30], in some cases through methylation of a transcription factor or cofactor [6, 25]. Histone arginine methylation is a component of the "histone code" that directs a variety of processes involving chromatin [31, 32]. For example, methylation of Arg3 of histone H4 by PRMT1 facilitates H4 acetylation and enhances transcription activation by nuclear hormone receptors in a synergistic fashion to CARM1 [8, 25, 33, 34].

PRMT1 is the predominant type I PRMT in mammalian cells, accounting for 85% of cellular PRMT activity [35, 36]. It is essential for early postimplantation development, as shown by the embryonic lethality of mouse *PRMT1*$^{-/-}$ mutants [36]. PRMT1 is expressed at detectible levels in all tissues examined [15–17, 36] (the highest is in developing neural structure in embryos [36]), and PRMT1 has been implicated in neuronal differentiation [37]. Besides the numerous substrates that interact with PRMT1, other proteins also bind to PRMT1. For example, antiproliferative protein interferon receptor IFNAR-1 [38] and BTG/TOB proteins [17, 39] bind PRMT1 and modulate its activity, and p160 nuclear hormone coactivators bind PRMT1 and recruit it to its substrate such as histone H4 [33].

PRMT1 gene is found in all eukaryotes tested and is highly conserved (Figure 1A). The sequence identity is over 90% among mammals, zebrafish, and *Xenopus*, and about 50% even between human and *S. cerevisiae*. There appears to be another gene closely related to PRMT1 genes both in *A. thaliana* and in human (HRMT1L3, XP_077339, on chromosome 12p13), which in each case shares 80% amino acid identity with PRMT1. Except for the N termini, the two genes have identical genomic structure: each pair has eight introns inserted at identical positions, and the locations of seven of those introns are also shared between human and *A. thaliana*. No function for this PRMT1-like gene has been reported. Like *S. cerevisiae*, *C. elegans* and *S. pombe* have only one copy of PRMT1 and share some of the splicing sites used by human and *A. thaliana*. *D. melanogaster* encodes four to six PRMT proteins of similar size, but of these only DmPRMT1 (AAF54556) has a high percentage

identity with the mammalian PRMT1 (65% vs. 15%–35% for the others; X.Z., unpublished observation).

The N terminus is the least conserved region among PRMT1s (Figure 1A). Three splicing variants (v1–v3) at the N terminus have been documented in human [15], producing mRNAs coding proteins between 353–371 amino acids long slightly different at their N termini [15, 36]. Variants v1 and v2 are also found in mouse, and v1 is found in rat. The two splicing variants of mouse are both expressed in all the tissues examined [36]. It has been reported that the 353 amino acid v1 and 371 amino acid v2 mouse PRMT1 have different substrate specificity [40]. By comparing available human PRMT1 ESTs with the genomic sequence (AC011495.1), at least three additional N-terminal splicing variants (v4–v6) can be identified (Figure 1B). In *Xenopus*, at least two versions corresponding to the mammalian v1 and v2 can also be found in the available EST sequences (BE025764 for v1; BE025704 for v2).

The vast majority of human and mouse ESTs represent splicing version 1, which encodes a protein of 353 amino acids. The wild-type PRMT1 we used is the rat PRMT1v1, which is identical to the mouse protein and differs from the human enzyme at only one position (H161 is Y in human). The previously reported human version 1 sequences (AAF62895 and CAA71765) lack the first ten amino acids of the rat sequence. However, close examination of the genomic sequence of human PRMT1 (AC011495.1) and of many ESTs (e.g., BE882188) suggests the presence of an additional exon that would add the same ten N-terminal amino acids to the human sequence. Here we present the structures of PRMT1-AdoHcy and its complex with peptide substrates, solved by molecular replacement using PRMT3 core structure [43]. These structures reveal active site residues, confirmed by mutagenesis studies, and indicate the locations of peptide binding channels. The oligomerization behavior of PRMT1, in solution and in crystal, is also discussed in comparison with the yeast RMT1 structure [44].

Results and Discussion

Overall Structure of PRMT1

We expressed the rat PRMT1v1 (353 amino acids) as a fusion protein containing a short N-terminal His tag (MGHHHHHH). The enzyme was very active using either hnRNP A1 (Figure 2A) or a 19 residue peptide (R3; Figure 2B) as substrate. Limited proteolysis using V8 or elastase resulted in very stable fragments lacking the first 10 or 13 residues, respectively (data not shown). His tag fusion proteins corresponding to these stable fragments (named M11 or S14) have similar enzymatic activity (Figure 2A, lanes 1–7) and form similar sizes of oligomers as the full length (Table 1). The deletions crystallized more readily than the full-length protein, and structures containing these two deletions or a full-length PRMT1 containing an E153Q mutation at the active site (see below) were determined (Table 2). All crystals contained the methylation product AdoHcy, and S14 and full-length E153Q also contained substrate peptide R3 (19 amino acids) or R1 (10 amino acids), respectively. They belong to the primitive tetragonal space group $P4_122$, though the cell dimensions vary slightly from crystal to crystal (Table 2). In all three structures only the residues after amino acid 40 were observed, suggesting a disordered amino terminus. There

are few significant structural differences among the three protein structures, and we describe primarily the ternary structure of S14-AdoHcy-R3 unless otherwise indicated.

The overall monomeric structure of PRMT1 can be divided into four parts (Figure 3A): N-terminal (red), AdoMet binding (green), β barrel (yellow), and dimerization arm (light blue). The AdoMet binding domain has the consensus fold conserved in other AdoMet-dependent methyltransferases [41, 42], whereas the β barrel domain is unique to the PRMT family [43]. Besides the N terminus (see below), the only size differences between PRMT1 and PRMT3 are in the β barrel domain—a single-residue deletion in the loop between strands β10 and β11 and an 8 residue insertion between strands β14 and β15 (Figure 3B). The additional 8 residues near the C terminus result in longer strands β14 and β15, while maintaining the exact position of the carboxyl group COO^- of the C-terminal residue next to the active site (Figure 3B). Interestingly, the position of the carboxyl terminus is also the same in the yeast RMT1 structure [44], which has an even larger insertion between strands β14 and β15 (see Figure 1A). This raises the possibility that the negatively charged C-terminal carboxyl group has an important role for binding positively charged substrate and/or for catalysis.

Cofactor Binding

The cofactor product, AdoHcy, which was present during crystal growth (see Experimental Procedures), is observed in a deep pocket on the carboxyl ends of the parallel strands β1–β5 (Figure 3A), surrounded by residues that are highly conserved in the PRMT family (Figure 4A). The interactions can be grouped according to the three moieties of AdoHcy: (1) the Gly-rich loop (G78 and G80) after strand β1 makes the backbone van der Waals contacts to the AdoHcy homocysteine and adenosine ribose moieties; (2) the acidic residue at the carboxyl end of strand β2 (E100) forms bifurcated hydrogen bonds with the ribose hydroxyl oxygens; and (3) the acidic residue from the loop after strand β3 (E129) hydrogen bonds with the amino group of adenine. These three interactions are conserved among many structurally characterized consensus AdoMet-dependent methyltransferases, and define the structural context of the AdoMet/AdoHcy binding site [41, 42]. Unique interactions for PRMT1 (and other members of the PRMT family) include H45 of helix αY (hydrogen bonding with one of the ribose hydroxyl oxygens), R54 of helix αZ (bridging the carboxylate groups of the AdoHcy homocysteine moiety and the active site residue E144), and flanking contacts to the AdoHcy adenine ring by C101 (after strand β2) and M155 and T158 (loop after strand β4).

The N-terminal region helps to constrain the bound AdoHcy. As noted above, the first 40 residues are neither conserved at the sequence level nor observed in the three structures, though in M11, residual density can be traced back to amino acid 36. In PRMT3 [43], an additional N-terminal helix αX was observed (Figures 1A and 3B). Without helix αX, the bound AdoHcy in PRMT1 appears more exposed to solvent. Helix αX contains 3 residues (YFxxY) invariant among all known PRMTs (Figure 1A), including F218 in PRMT3 that forms an edge-to-face hydrophobic interaction with the adenine ring of AdoHcy, and Y217 and Y221, whose hydroxyl groups point to the active site residue E335 (Figure 4B) [43]. In PRMT1, deleting helix αX (deletion mutant S38 in Table 1) indeed reduced cofactor

crosslinking (Figure 2D, lane 4) and abolished enzymatic activity (Figure 2A, lanes 9 and 10), suggesting important roles of helix αX both in cofactor binding and catalysis.

PRMT Dimerization Is Essential for AdoMet Binding and Enzymatic Activity

A hydrophobic dimer interface (Figure 5) identical to that of the PRMT3 core [43] and yeast RMT1 [44] is observed in PRMT1, despite very different crystallization conditions, space group, and cell dimensions. This observation supports the notion that dimer formation is a conserved feature in the PRMT family [43]. A mutant ΔARM that lacks the entire dimerization arm (residues 188–222) was generated. The purified ΔARM protein eluted as a 37 kDa monomer protein from a gel filtration column (Table 1). The ΔARM mutant completely lacks enzymatic activity (Figure 2A, lane 25), most likely because it is unable to bind cofactor AdoMet as determined by UV crosslinking experiments (Figure 2C, and Figure 2D, lane 11). A similar mutant of yeast RMT1 that replaces the arm with alanines also resulted in the loss of dimer formation and methylation activity [44]. In the crystal structure, the dimer interface is formed between the arm and the outer surface of the AdoMet binding site (Figure 5C). It is conceivable that the dimer interaction is required to engage the residues on the other side of the structural elements (αY-loop-αZ and β1-loop-αA) to interact with AdoMet properly.

Another potential function of the conserved PRMT dimer might be to allow processive production of the final methylation product, asymmetric dimethylarginine. PRMT substrates isolated in vivo are usually completely or nearly completely dimethylated [3, 4, 45–47]. It has been shown in vitro that PRMT6 forms dimethylarginine in a processive manner [20]. It is conceivable that a ring-like dimer could allow the product of the first methylation reaction, monomethylarginine, to enter the active site of the second molecule of the dimer, without releasing the substrate from the ring or replenishing the methyl donor.

In addition to the dimer interaction, we also observed a disulfide bond between C254 from strand β9 of two crystallographically related molecules. This interaction caused PRMT1 dimers to form an extended polymer in the crystal lattice (Figure 5A). The recombinant PRMT1 protein existed as an oligomer as judged by gel filtration chromatography and dynamic light scattering (Table 1). However, yeast RMT1 exists mainly as a dimer in solution but forms a hexamer (a trimer of three dimers) in the crystal lattice [44]. We note that the higher order oligomerization does not occur in the absence of dimerization (i.e., in the case of ΔARM). However, a C254S mutant still forms oligomers similar to wild-type (Table 1), and fully retains both cofactor binding (Figure 2D, lane 10) and methylation activity (Figure 2A, lane 24). This is consistent with the fact that C254 is not completely conserved among PRMT1s. Either the C254 disulfide bond does not contribute to oligomerization of PRMT1 in solution and is unique to the crystal lattice, or the disulfide bond is one of several redundant stabilizing contacts.

Substrate Binding Surface

The peptides that contain one or three copies of the consensus RGG repeat sequence (R1 or R3, respectively) were cocrystallized with PRMT1. As shown in Figure 2B, the R3 peptide is a very good substrate for PRMT1 (lanes 7–11) and competes with a protein substrate

hnRNP A1 effectively (lanes 1–6). In contrast, the R1 peptide competes poorly with hnRNP A1 (lanes 12–17), and was barely methylated under similar conditions (data not shown).

The substrate binding surface of PRMT1 is expected to be acidic, because most substrates for PRMT1 contain multiple arginines. As shown in the surface charge distribution of PRMT1 dimer (Figure 5B), acidic residues are enriched on the inner surface of the dimer ring and the outer surface of the β barrel. The structure of the ternary S14-AdoHcy-R3 complex included electron densities revealing the location of bound peptide ligands (Figure 6). However, the densities were broken into three separate peptide fragment binding sites (P1, P2, and P3), and, except for the arginine in the active site, the side chain densities were not sufficiently resolved to allow clear identification of the amino acids. In comparison, no density was observed in any of the three P sites in the structure of M11-AdoHcy without peptide.

The three disconnected densities probably represent a mixture of binding modes of R3 peptide, which contains three potential methylation targets at positions 3, 9, and 15. Sites P1 and P2 correspond to the acidic grooves in the interface between the two domains (green and yellow in Figure 6B). P1 is along the edge of helices αY (red) and αZ (green) and next to strand β11 and the THW loop (Figure 6B). P2 is flanked by helix αD (green) and the short 3_{10} helix αI as well as the loop between β13 and β14 (yellow). If the central Arg9 were the target bound in the active site, connecting peptide binding sites P1 and P2 would cover the active site and the entire length of the peptide (Figure 6C). The densities immediately around the active site arginine are not observed, and the gaps account for the two glycines flanking the arginine. Due to the ambiguous nature of the density, the peptide can be fitted equally well in either linear orientation. The acidic grooves containing P1 and P2 are almost parallel to the N-terminal helices αY (Figure 6B) and αX (if present analogously to the PRMT3 structure), respectively. It is conceivable that the rest of the N-terminal sequences differing among PRMT1 splicing variants could also be in the vicinity to contact the protein substrate occupying the P2 binding groove, consistent with the observation that PRMT1 splicing variants have different substrate specificity [40].

Site P3 corresponds to one of the grooves (Figure 6D) perpendicular to the sheet formed by β strands 9, 13, 14, and 15 (see Figure 3A). When the end arginine (either Arg3 or Arg15) is bound in the active site, connection of peptide binding sites P2 and P3 would account for the length of the whole peptide (Figure 6D). Additional acidic grooves running parallel to site P3 can be identified. These grooves could form additional binding sites for protein substrate with more RGG repeats.

In the case of R1 peptide, which is a poor substrate, no density was observed in the active site or the peptide binding sites P1 and P2 in the structure of the E153Q-AdoHcy-R1 ternary complex. However, we did observe residual, broken density in the peptide binding site P3 (not shown), which is away from the active site. Perhaps the preferential binding to this nonproductive site is the cause for R1 peptide being a poor substrate. Alternatively, E153Q mutation could prevent stable binding of the peptide in the active site.

Active Site

The target arginine is situated in a deep pocket between the AdoMet binding domain and the β barrel domain (Figure 6A). The residues that make up the active site are conserved across the PRMT family, and form a hairpin between strand β4 and helix αD. This is called the "double-E loop" because it contains two invariant glutamates (E144 and E153; Figure 1A). The hydrophobic methylene groups of the target arginine lie parallel to the plane of the Y148 aromatic ring, while the side chain of E144 and the main chain carbonyl oxygen of E153 hydrogen bond the guanidino group (Figure 7A).

Surprisingly, the side chain of E153 points away from, rather than toward, the bound guanidino group in the active site. We noted that all three forms of PRMT1 were crystallized at low pH (~4.7); under this condition PRMT1 is inactive (Figure 7C), perhaps due to protonation of one or both Glu side chains. Consistent with the effects of protonation, E153Q mutation abolished methylation activity (Figure 2A, lane 16; Table 1), whereas the E153D mutation reduced the activity to about 0.03% (Figure 2A, lane 17; Table 1). Both E153 mutants (D and Q) oligomerized to about the same size as the wild-type (Table 1), indicating that the mutations did not affect the overall structural integrity of the protein. On the other hand, regarding the second glutamate in the double-E loop, both E144 mutants (particularly E144Q) are more aggregated (Table 1), suggesting that the mutations may cause some structural perturbation by interrupting E144-R54 interaction (Figures 4A and 7A), and the activities of E144Q and E144D mutants were reduced by 3000- and 10-fold, respectively (Figure 2A, lanes 18–20; Table 1). This strongly suggests that the negative charges on both E153 and E144 are critical for catalysis, while the length of the side chain (Glu vs. Asp) is also important.

We superimposed the active site residues of PRMT1 onto PRMT3, which was crystallized at pH ~6.3 [43] where PRMT3 has detectable activity (Figure 7C). As shown in Figure 7B, the largest deviation is between E153 and S154 of PRMT1 and the corresponding residues E335 and S336 of PRMT3. The superimposition placed the target arginine in between E326 and E335 of PRMT3; the side chain of E335 could form a bifurcated hydrogen bond with the guanidino group (Figure 7B). A network of charge-charge interactions involving E335, the target arginine, E326, R236, and the AdoHcy carboxylate would place the target nitrogen atom and the sulfur atom of AdoHcy into close proximity (shown by an arrow in Figure 7B). It has been proposed that the interaction with E335 of PRMT3 (equivalent to E153 of PRMT1) redistributes the positive charge on the guanidino group toward one amino group while leaving a lone pair of electrons on the other amino group to attack the cationic methylsulfonium moiety of AdoMet [43]. The corresponding mutant of this residue in CARM1 (E267Q) has been used to demonstrate that the methyltransferase activity of CARM1 was required for synergy among nuclear receptor coactivators [48].

Biological Implications

We have described the crystal structures of the predominant protein arginine methyltransferase PRMT1, in the presence of methylation product AdoHcy and/or the peptide substrate containing either one or three target arginines. PRMT1 forms a ring-like dimer essential for AdoMet binding and enzymatic activity. The structure also reveals

residues for catalysis (E153Q) and candidate residues for substrate recognition along three grooves (P1, P2, and P3). This structure provides useful starting points to map residues important for the binding of PRMT1 to its diverse protein substrates as well as other binding partners.

Experimental Procedures

Protein Expression and Purification

Rat PRMT1 gene was subcloned from the original GST-PRMT1 construct [17] by PCR into a modified pET28b (Novagen) vector, which adds a short N-terminal MGHHHHHH tag and accepts an NdeI-EcoRI insert. Deletions and point mutations were constructed by PCR using the same vector. Cultures of *E. coli* strain BL21(DE3) containing PRMT1 constructs were grown at 37°C to OD_{600} = 0.4, shifted to 22°C, and induced by 0.4 mM IPTG overnight at 22°C.

The His-tagged proteins were purified using Ni-chelating, Mono Q, and Sephacryl S300 columns (Amersham-Pharmacia). One hundred micromolar AdoHcy was incubated with the load samples of the Mono Q and S300 columns prior to chromatography. The proteins were homogeneous as judged by overloaded SDS-PAGE stained with Coomassie blue and their concentrations were estimated by OD_{280} absorption using a calculated extinction coefficient of 52,090 $M^{-1}cm^{-1}$.

Nontagged proteins were expressed using vector pET29b (Novagen). The proteins were purified using two consecutive runs of Hitrap Q column, a Resource Q column, a 200HR Sephadex or S300 Sephacryl gel filtration column, followed by a Mono Q column (all Amersham-Pharmacia). During early steps of purification, PRMT activity using hnRNP A1 as substrate was determined. The full-length protein without tag and the S14 with His tag were both expressed poorly in *E. coli* (<20% of the others) for unknown reasons, although the majority of all expressed proteins was soluble. For comparison, the yield of full-length protein (plasmid pXC246) was about 0.4 mg/L with a final purity of about 80%, while the yield of the M11 deletion mutant (plasmid pXC247) was about 4 mg/L and >95% pure as judged by SDS-PAGE.

PRMT Activity Assay, UV Crosslinking, and Oligomerization

PRMT activity was assayed as described [43]. For UV crosslinking, 20 μl of PRMT1 (1–5 μg) was incubated with 0.5 μCi of [methyl-^{3}H]AdoMet (78 Ci/mmol, NEN NET155H) overnight at 4°C. Samples were added to a 96-well plate and placed 8 cm from an upside-down UV transilluminator (VWR, 302 nm) for various times. The proteins were then separated by SDS-PAGE, stained with Coomassie blue, and subjected to fluorography.

The protein size (oligomerization) was determined by gel filtration chromatography on a Sephacryl S300 column using proteins (>0.5 mg/ml) preincubated with AdoHcy. The column buffer contained 20 mM Tris (pH 8.0), 250 mM NaCl, 1 mM EDTA, 0.1% 2-mercaptoethanol, and 5% glycerol. Size was estimated based on a standard run under the same buffer condition. The protein size was also determined by dynamic light scattering

using DynaPro Molecular Sizing Instrument (Protein Solutions), at 1 mg/ml of protein concentration. The size shown in Table 1 was calculated with a regularization model.

Crystallography

The proteins were concentrated to about 20 mg/ml in the gel filtration column buffer with 600 μM of AdoHcy. Crystals were obtained via the hanging drop method, with the mother liquor containing 100 mM Tris (pH 9.0) and 1.6 M ammonium phosphate monobasic (final pH ~4.7). The concentration of peptide was 1 mM when present.

Complete data sets were collected at the beamlines X26C (wavelength 1.1 Å, ADSC Q4) and X12C (wavelength 1.1 Å, Brandeis B2) of the National Synchrotron Light Source, Brookhaven National Laboratory (Table 2). The structures were solved by molecular replacement using the refined PRMT3 core structure [43] as the search model, using AMoRe [49]; the resulting models were refined using X-PLOR [50]. Electron densities corresponding to the peptides were established in the difference Fourier annealed omit maps.

Acknowledgments

We thank Dr. Harvey R. Herschman (UCLA) for providing the construct to express the GST-PRMT1 fusion, Dr. Adrian Krainer (Cold Spring Harbor Laboratory) for providing the construct to express hnRNP A1, Susan Sunay for technical assistance during protein purification and crystallization, Paul Kearney for mutagenesis, Dr. Lan Zhou for help with X-ray data collection and molecular replacement, and Dr. Robert M. Blumenthal (Medical College of Ohio) for critical comments on the manuscript. These studies were supported in part by the National Institutes of Health (GM61355).

References

1. Lee HW, Kim S, Paik WK. S-adenosylmethionine: protein-arginine methyltransferase. Purification and mechanism of the enzyme Biochemistry. 1977; 16:78–85.
2. Gary JD, Clarke S. RNA and protein interactions modulated by protein arginine methylation. Prog Nucleic Acid Res Mol Biol. 1998; 61:65–131. [PubMed: 9752719]
3. Smith JJ, Rucknagel KP, Schierhorn A, Tang J, Nemeth A, Linder M, Herschman HR, Wahle E. Unusual sites of arginine methylation in poly(A)-binding protein II and in vitro methylation by protein arginine methyltransferases PRMT1 and PRMT3. J Biol Chem. 1999; 274:13229–13234. [PubMed: 10224081]
4. Klein S, Carroll JA, Chen Y, Henry MF, Henry PA, Ortonowski IE, Pintucci G, Beavis RC, Burgess WH, Rifkin DB. Biochemical analysis of the arginine methylation of high molecular weight fibroblast growth factor-2. J Biol Chem. 2000; 275:3150–3157. [PubMed: 10652299]
5. Tang J, Kao PN, Herschman HR. Protein-arginine methyltransferase I, the predominant protein-arginine methyltransferase in cells, interacts with and is regulated by interleukin enhancer-binding factor 3. J Biol Chem. 2000; 275:19866–19876. [PubMed: 10749851]
6. Mowen KA, Tang J, Zhu W, Schurter BT, Shuai K, Herschman HR, David M. Arginine methylation of STAT1 modulates IFNα/β-induced transcription. Cell. 2001; 104:731–741. [PubMed: 11257227]
7. Strahl BD, Briggs SD, Brame CJ, Caldwell JA, Koh SS, Ma H, Cook RG, Shabanowitz J, Hunt DF, Stallcup MR, et al. Methylation of histone H4 at arginine 3 occurs in vivo and is mediated by the nuclear receptor coactivator PRMT1. Curr Biol. 2001; 11:996–1000. [PubMed: 11448779]
8. Wang H, Huang ZQ, Xia L, Feng Q, Erdjument-Bromage H, Strahl BD, Briggs SD, Allis CD, Wong J, Tempst P, et al. Methylation of histone H4 at arginine 3 facilitating transcriptional activation by nuclear hormone receptor. Science. 2001; 293:853–857. [PubMed: 11387442]
9. Wada K, Inoue K, Hagiwara M. Identification of methylated proteins by protein arginine N-methyltransferase 1, PRMT1, with a new expression cloning strategy. Biochim Biophys Acta. 2002; 1591:1–10. [PubMed: 12183049]

10. Henry MF, Silver PA. A novel methyltransferase (Hmt1p) modifies poly(A)$^+$-RNA-binding proteins. Mol Cell Biol. 1996; 16:3668–3678. [PubMed: 8668183]
11. Gary JD, Lin WJ, Yang MC, Herschman HR, Clarke S. The predominant protein-arginine methyltransferase from *Saccharomyces cerevisiae*. J Biol Chem. 1996; 271:12585–12594. [PubMed: 8647869]
12. Abramovich C, Yakobson B, Chebath J, Revel M. A protein-arginine methyltransferase binds to the intra-cytoplasmic domain of the IFNAR1 chain in the type I interferon receptor. EMBO J. 1997; 16:260–266. [PubMed: 9029147]
13. Chen D, Ma H, Hong H, Koh SS, Huang SM, Schurter BT, Aswad DW, Stallcup MR. Regulation of transcription by a protein methyltransferase. Science. 1999; 284:2174–2177. [PubMed: 10381882]
14. Katsanis N, Yaspo ML, Fisher EM. Identification and mapping of a novel human gene, HRMT1L1, homologous to the rat protein arginine N-methyltransferase 1 (PRMT1) gene. Mamm Genome. 1997; 8:526–529. [PubMed: 9196002]
15. Scott HS, Antonarakis SE, Lalioti MD, Rossier C, Silver PA, Henry MF. Identification and characterization of two putative human arginine methyltransferases (HRMT1L1 and HRMT1L2). Genomics. 1998; 48:330–340. [PubMed: 9545638]
16. Tang J, Gary JD, Clarke S, Herschman HR. PRMT 3, a type I protein arginine N-methyltransferase that differs from PRMT1 in its oligomerization, subcellular localization, substrate specificity, and regulation. J Biol Chem. 1998; 273:16935–16945. [PubMed: 9642256]
17. Lin WJ, Gary JD, Yang MC, Clarke S, Herschman HR. The mammalian immediate-early TIS21 protein and the leukemia-associated BTG1 protein interact with a protein-arginine N-methyltransferase. J Biol Chem. 1996; 271:15034–15044. [PubMed: 8663146]
18. Lee JH, Cook JR, Pollack BP, Kinzy TG, Norris D, Pestka S. Hsl7p, the yeast homologue of human JBP1, is a protein methyltransferase. Biochem Biophys Res Commun. 2000; 274:105–111. [PubMed: 10903903]
19. Pollack BP, Kotenko SV, He W, Izotova LS, Barnoski BL, Pestka S. The human homologue of the yeast proteins Skb1 and Hsl7p interacts with Jak kinases and contains protein methyltransferase activity. J Biol Chem. 1999; 274:31531–31542. [PubMed: 10531356]
20. Frankel A, Yadav N, Lee J, Branscombe TL, Clarke S, Bedford MT. The novel human protein arginine N-methyltransferase PRMT6 is a nuclear enzyme displaying unique substrate specificity. J Biol Chem. 2002; 277:3537–3543. [PubMed: 11724789]
21. Rajpurohit R, Paik WK, Kim S. Effect of enzymic methylation of heterogeneous ribonucleoprotein particle A1 on its nucleic-acid binding and controlled proteolysis. Biochem J. 1994; 304:903–909. [PubMed: 7818496]
22. Valentini SR, Weiss VH, Silver PA. Arginine methylation and binding of Hrp1p to the efficiency element for mRNA 3′-end formation. RNA. 1999; 5:272–280. [PubMed: 10024178]
23. Raman B, Guarnaccia C, Nadassy K, Zakhariev S, Pintar A, Zanuttin F, Frigyes D, Acatrinei C, Vindigni A, Pongor G, et al. N(Ω)-arginine dimethylation modulates the interaction between a Gly/Arg-rich peptide from human nucleolin and nucleic acids. Nucleic Acids Res. 2001; 29:3377–3384. [PubMed: 11504875]
24. Bedford MT, Frankel A, Yaffe MB, Clarke S, Leder P, Richard S. Arginine methylation inhibits the binding of proline-rich ligands to Src homology 3, but not WW, domains. J Biol Chem. 2000; 275:16030–16036. [PubMed: 10748127]
25. Xu W, Chen H, Du K, Asahara H, Tini M, Emerson BM, Montminy M, Evans RM. A transcriptional switch mediated by cofactor methylation. Science. 2001; 294:2507–2511. [PubMed: 11701890]
26. Pintucci G, Quarto N, Rifkin DB. Methylation of high molecular weight fibroblast growth factor-2 determines post-translational increases in molecular weight and affects its intracellular distribution. Mol Biol Cell. 1996; 7:1249–1258. [PubMed: 8856668]
27. Shen EC, Henry MF, Weiss VH, Valentini SR, Silver PA, Lee MS. Arginine methylation facilitates the nuclear export of hnRNP proteins. Genes Dev. 1998; 12:679–691. [PubMed: 9499403]

28. Yun CY, Fu XD. Conserved SR protein kinase functions in nuclear import and its action is counteracted by arginine methylation in *Saccharomyces cerevisiae*. J Cell Biol. 2000; 150:707–718. [PubMed: 10952997]
29. Nichols RC, Wang XW, Tang J, Hamilton BJ, High FA, Herschman HR, Rigby WF. The RGG domain in hnRNP A2 affects subcellular localization. Exp Cell Res. 2000; 256:522–532. [PubMed: 10772824]
30. Aletta JM, Cimato TR, Ettinger MJ. Protein methylation: a signal event in post-translational modification. Trends Biochem Sci. 1998; 23:89–91. [PubMed: 9581497]
31. Strahl BD, Allis CD. The language of covalent histone modifications. Nature. 2000; 403:41–45. [PubMed: 10638745]
32. Kouzarides T. Histone methylation in transcriptional control. Curr Opin Genet Dev. 2002; 12:198–209. [PubMed: 11893494]
33. Stallcup MR, Chen D, Koh SS, Ma H, Lee Y, Li H, Schurter BT, Aswad DW. Co-operation between protein-acetylating and protein-methylating co-activators in transcriptional activation. Biochem Soc Trans. 2000; 28:415–418. [PubMed: 10961931]
34. Strahl BD, Briggs SD, Brame CJ, Caldwell JA, Koh SS, Ma H, Cook RG, Shabanowitz J, Hunt DF, Stallcup MR, et al. Methylation of histone H4 at arginine 3 occurs in vivo and is mediated by the nuclear receptor coactivator PRMT1. Curr Biol. 2001; 11:996–1000. [PubMed: 11448779]
35. Tang J, Frankel A, Cook RJ, Kim S, Paik WK, Williams KR, Clarke S, Herschman HR. PRMT1 is the predominant type I protein arginine methyltransferase in mammalian cells. J Biol Chem. 2000; 275:7723–7730. [PubMed: 10713084]
36. Pawlak MR, Scherer CA, Chen J, Roshon MJ, Ruley HE. Arginine N-methyltransferase 1 is required for early postimplantation mouse development, but cells deficient in the enzyme are viable. Mol Cell Biol. 2000; 20:4859–4869. [PubMed: 10848611]
37. Cimato TR, Tang J, Xu Y, Guarnaccia C, Herschman HR, Pongor S, Aletta JM. Nerve growth factor-mediated increases in protein methylation occur predominantly at type I arginine methylation sites and involve protein arginine methyltransferase 1. J Neurosci Res. 2002; 67:435–442. [PubMed: 11835310]
38. Altschuler L, Wook JO, Gurari D, Chebath J, Revel M. Involvement of receptor-bound protein methyltransferase PRMT1 in antiviral and antiproliferative effects of type I interferons. J Interferon Cytokine Res. 1999; 19:189–195. [PubMed: 10090404]
39. Berthet C, Guehenneux F, Revol V, Samarut C, Lukaszewicz A, Dehay C, Dumontet C, Magaud JP, Rouault JP. Interaction of PRMT1 with BTG/TOB proteins in cell signalling: molecular analysis and functional aspects. Genes Cells. 2002; 7:29–39. [PubMed: 11856371]
40. Pawlak MR, Banik-Maiti S, Pietenpol JA, Ruley HE. Protein arginine methyltransferase I: substrate specificity and role in hnRNP assembly. J Cell Biochem. 2002; 87:394–407. [PubMed: 12397599]
41. Fauman, EB.; Blumenthal, RM.; Cheng, X. Structure and evolution of Adomet-dependent methyltransferases. In: Cheng, X.; Blumenthal, RM., editors. S-Adenosylmethionine-Dependent Methyltransferases: Structures and Functions. River Edge, NJ: World Scientific; 1999. p. 1-38.
42. Cheng X, Roberts RJ. AdoMet-dependent methylation, DNA methyltransferases and base flipping. Nucleic Acids Res. 2001; 29:3784–3795. [PubMed: 11557810]
43. Zhang X, Zhou L, Cheng X. Crystal structure of the conserved core of protein arginine methyltransferase PRMT3. EMBO J. 2000; 19:3509–3519. [PubMed: 10899106]
44. Weiss VH, McBride AE, Soriano MA, Filman DJ, Silver PA, Hogle JM. The structure and oligomerization of the yeast arginine methyltransferase, Hmt1. Nat Struct Biol. 2000; 7:1165–1171. [PubMed: 11101900]
45. Kim S, Merrill BM, Rajpurohit R, Kumar A, Stone KL, Papov VV, Schneiders JM, Szer W, Wilson SH, Paik WK, et al. Identification of N(G)-methylarginine residues in human heterogeneous RNP protein A1: Phe/Gly-Gly-Gly-Arg-Gly-Gly-Gly/Phe is a preferred recognition motif. Biochemistry. 1997; 36:5185–5192. [PubMed: 9136880]
46. Lischwe MA, Cook RG, Ahn YS, Yeoman LC, Busch H. Clustering of glycine and NG, NG-dimethylarginine in nucleolar protein C23. Biochemistry. 1985; 24:6025–6028. [PubMed: 4084504]

47. Lischwe MA, Ochs RL, Reddy R, Cook RG, Yeoman LC, Tan EM, Reichlin M, Busch H. Purification and partial characterization of a nucleolar scleroderma antigen (Mr = 34,000; pI, 8.5) rich in NG, NG-dimethylarginine. J Biol Chem. 1985; 260:14304–14310. [PubMed: 2414294]

48. Lee YH, Koh SS, Zhang X, Cheng X, Stallcup MR. Synergy among nuclear receptor coactivators: selective requirement for protein methyltransferase and acetyltransferase activities. Mol Cell Biol. 2002; 22:3621–3632. [PubMed: 11997499]

49. Navaza J. Implementation of molecular replacement in AMoRe. Acta Crystallogr D. 2001; 57:1367–1372. [PubMed: 11567147]

50. Brünger, AT. A System for X-Ray Crystallography and NMR. New Haven: Yale University; 1992. X-PLOR.

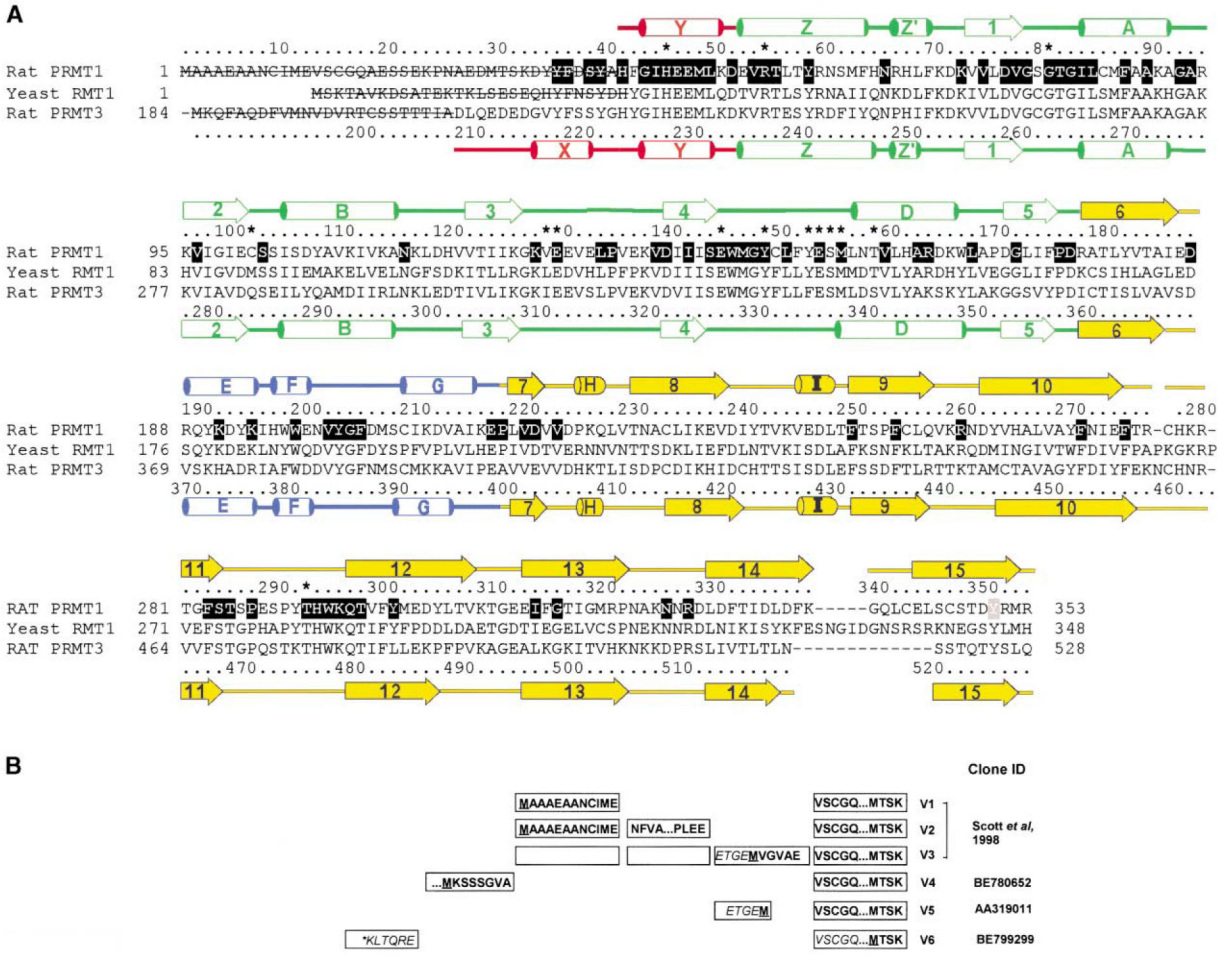

Figure 1. Members of the PRMT1 Family

(A) Structure-based sequence alignment of rat PRMT1, PRMT3 [43], and yeast RMT1 [44]. Letters (A–Z) for helices and numbers (1–15) for strands indicate the secondary structure elements of rat PRMT1 or PRMT3; residue numbering is shown above or below the sequences. The color coding is red for the N terminus including helix αY (residues 41–51), green for the AdoMet binding domain (residues 52–176), yellow for the β barrel structure (residues 177–187 and 217–352), and blue for the dimerization arm (residues 188–216). For rat PRMT1, the amino acids highlighted (white against black) are invariant among PRMT1s from various organisms: rat PRMT1 (GenBank accession number NP_077339), human PRMT1-v2 (modified from CAA71764), PRMT1-like (also called HMT1L3, XP_006990), *C. elegans* PRMT1 (CAB54335), *D. melanogaster* PRMT1 (AAF54556), *A. thaliana* PRMT1 (CAB79709), *A. thaliana* PRMT1-like (AAC62148), *S. pombe* PRMT1 (CAB63498), and *S. cerevisiae* RMT1 (585608). The *Xenopus* and zebrafish PRMT1 sequences were assembled from ESTs with sequences highly similar to that of rat PRMT1. The N-terminal sequences shown with a strikethrough are not observed in the crystal structures, presumably due to being highly disordered in the crystals. The asterisks above the sequence indicate residues important for cofactor binding (see Figure 4A) and/or catalysis (see Figure 7A).

(B) N-terminal splicing variants of human PRMT1.

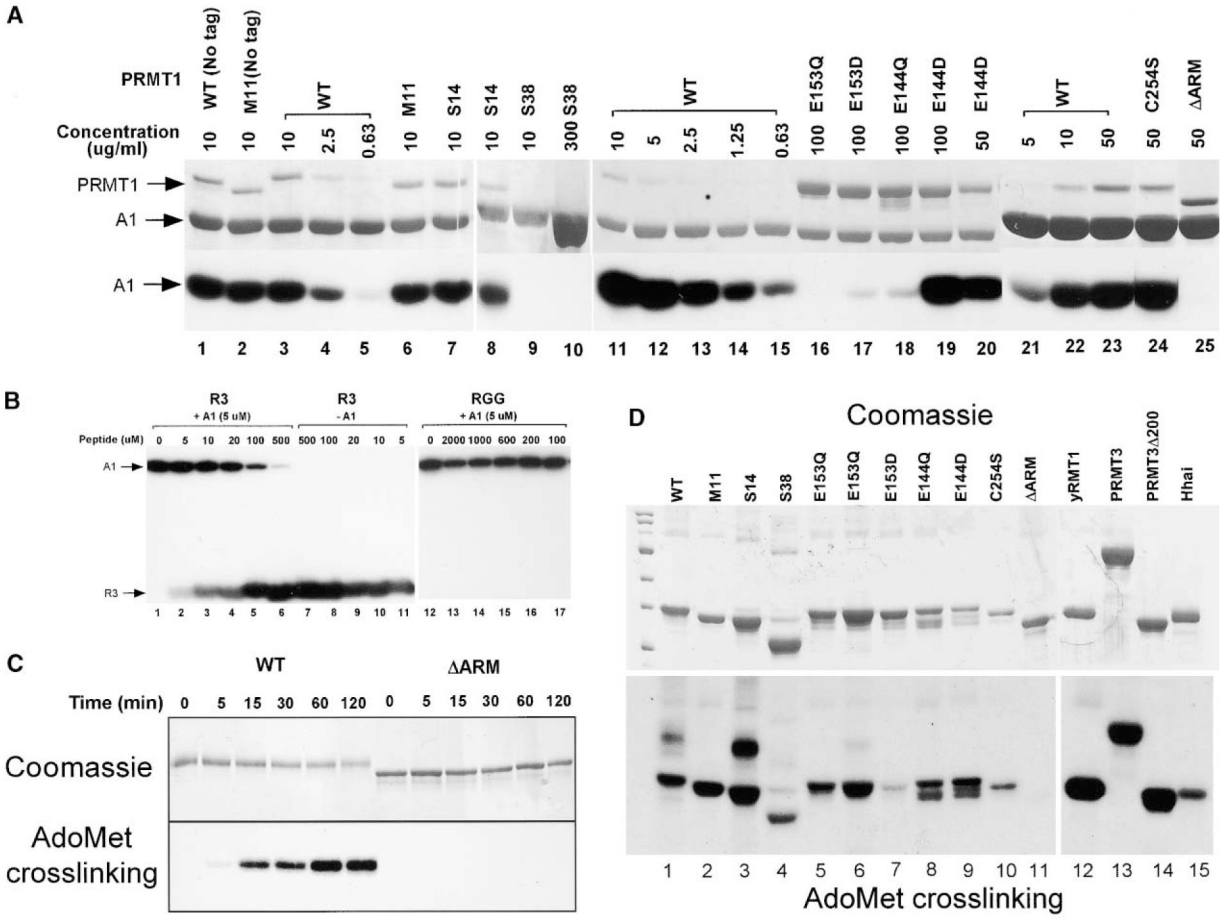

Figure 2. Activity of PRMT1 Proteins

(A) Reactions (20 μl) contained 4 or 8 μM of purified hnRNP A1 (130 or 260 μg/ml), 40 μM [methyl-^{3}H]AdoMet (0.5 μCi), and the indicated amount of PRMT1 in 100 mM Tris (pH 8.0), 200 mM NaCl, 2 mM EDTA, and 1 mM dithiothreitol. After incubating at 37°C for 15 min, the samples were analyzed by SDS-PAGE. The upper panel shows the Coomassie-stained gel of total PRMT1 and hnRNP A1, while the lower panel shows the image resulting from fluorography. Various amounts of wild-type PRMT1 (lanes 3–5, 11–15, and 21–23) were used so that the relative activity of mutant PRMTs could be estimated.

(B) Methylation of peptides R3 or R1 (RGG) and competition by hnRNP A1. Reaction conditions are identical to Figure 2A and include 10 μg/ml of PRMT1, 5 μM of hnRNP A1 and/or various amounts of peptides as indicated.

(C) Time course of AdoMet crosslinking of wild-type PRMT1 and ΔARM mutant.

(D) AdoMet crosslinking of various PRMTs and mutants. The samples were treated with UV for 1 hr. Controls were used: yRMT1 (yeast RMT1), PRMT3 (full-length rat PRMT3), PRMT3Δ200 (rat PRMT3 conserved core), and HhaI (DNA cytosine methyltransferase).

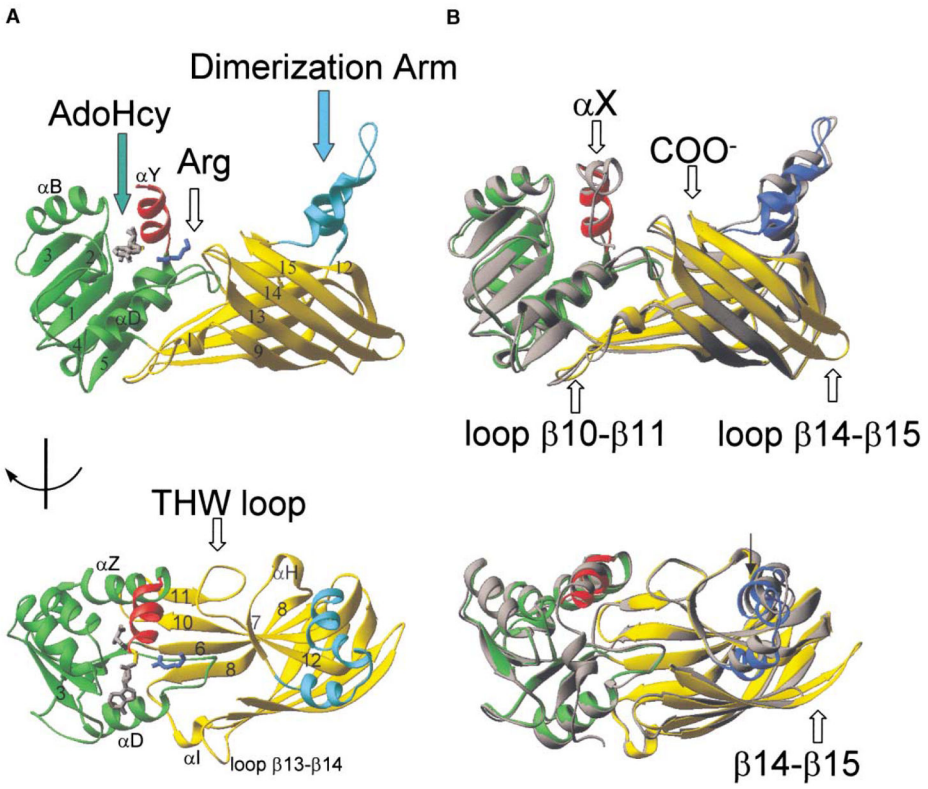

Figure 3. Structure of PRMT1

(A) Two views (top and bottom panels) of monomer structure. The N-terminal helix αY is shown in red, and the AdoMet binding domain in green. The bound AdoHcy is shown in a stick model with the sulfur atom (where the transferable methyl group would be attached in AdoMet) shown in yellow. The β barrel structure is shown in yellow, and the dimerization arm (which is inserted into the β barrel) is in light blue (see Figure 1A). The bound arginine (blue) in the S14-AdoHcy-R3 ternary complex defines the active site, located between the AdoMet binding domain (green) and the β barrel (yellow).

(B) Superposition of PRMT1 (residues 41–353, colored according to Figure 1A) and PRMT3 core (residues 208–528, in gray). Besides deletion or insertion (located in loops between β10 and β11 and between β14 and β15), the two structures can be superimposed with less than 1 Å of root-mean-square deviation between them.

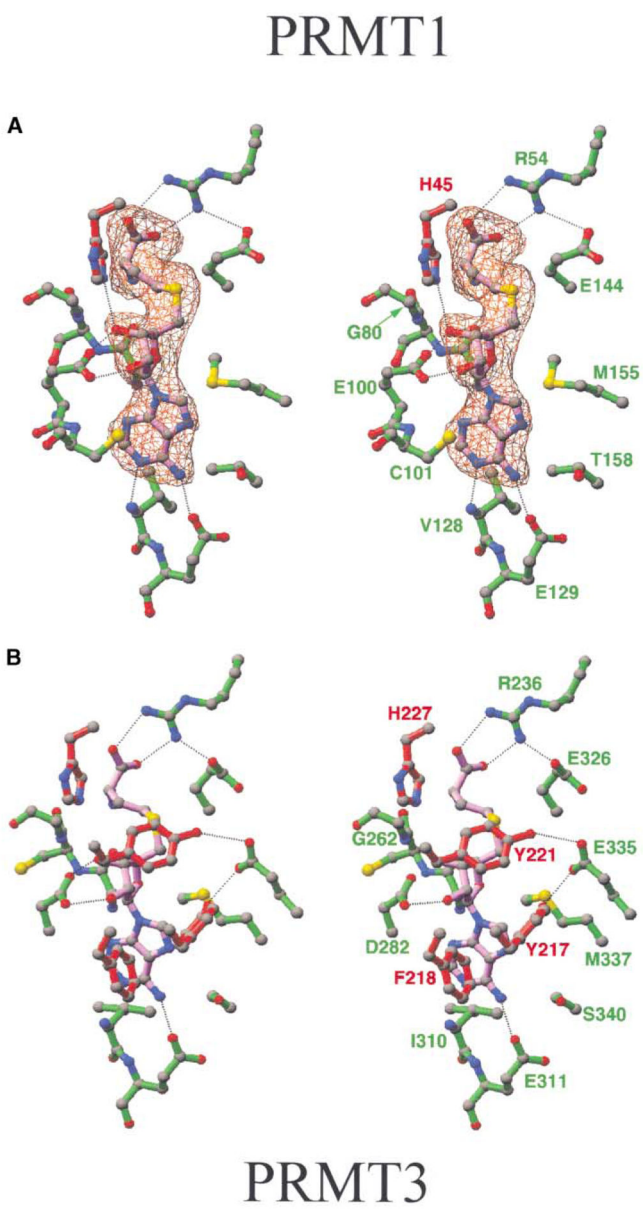

Figure 4. Stereo View of AdoHcy Binding

A) In PRMT1, the difference electron density map is contoured at 5.5σ. Dashed lines indicate hydrogen bonds.

(B) In PRMT3 (PDB ID code 1F3J; [43]), the corresponding N-terminal residues F218, Y217, and Y221 (red) are not observed in the PRMT1 structure.

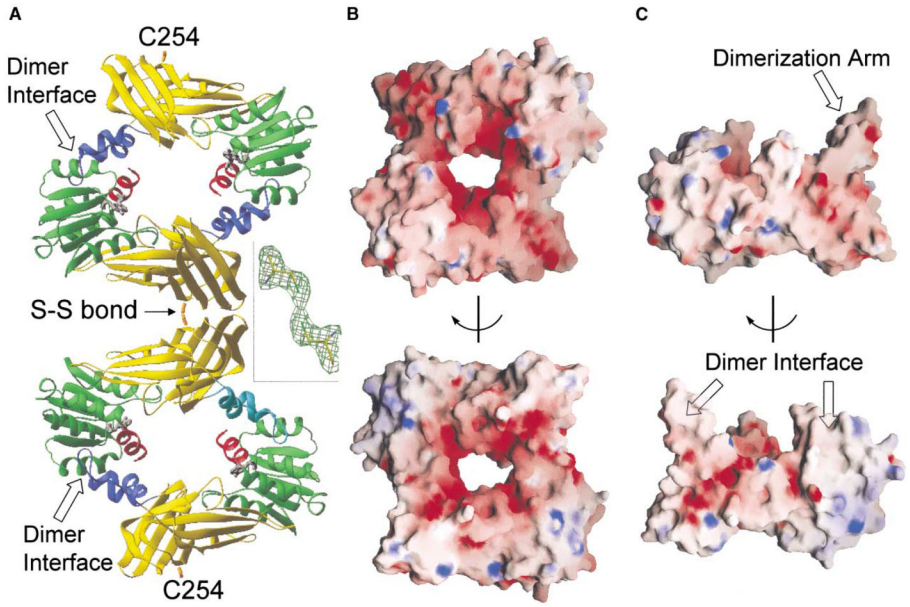

Figure 5. Dimer Formation of PRMT1

(A) Two ring-like dimers (related by a crystallographic 2-fold) connected by a surface C254 via a disulfide bond are shown with a difference electron density map contoured at 5.5σ. The dimer is formed through the arm (blue) and the outer surface of AdoMet binding domain (green), as indicated. The AdoHcy (gray) is in a stick model.

(B) Two opposite GRASP surfaces of PRMT1 dimer. The surface is colored red for negative, blue for positive, and white for neutral.

(C) Two opposite GRASP surfaces of PRMT1 monomer. Dimerization is mediated through hydrophobic patches of the arm and the outer surface of AdoMet binding domain, as indicated.

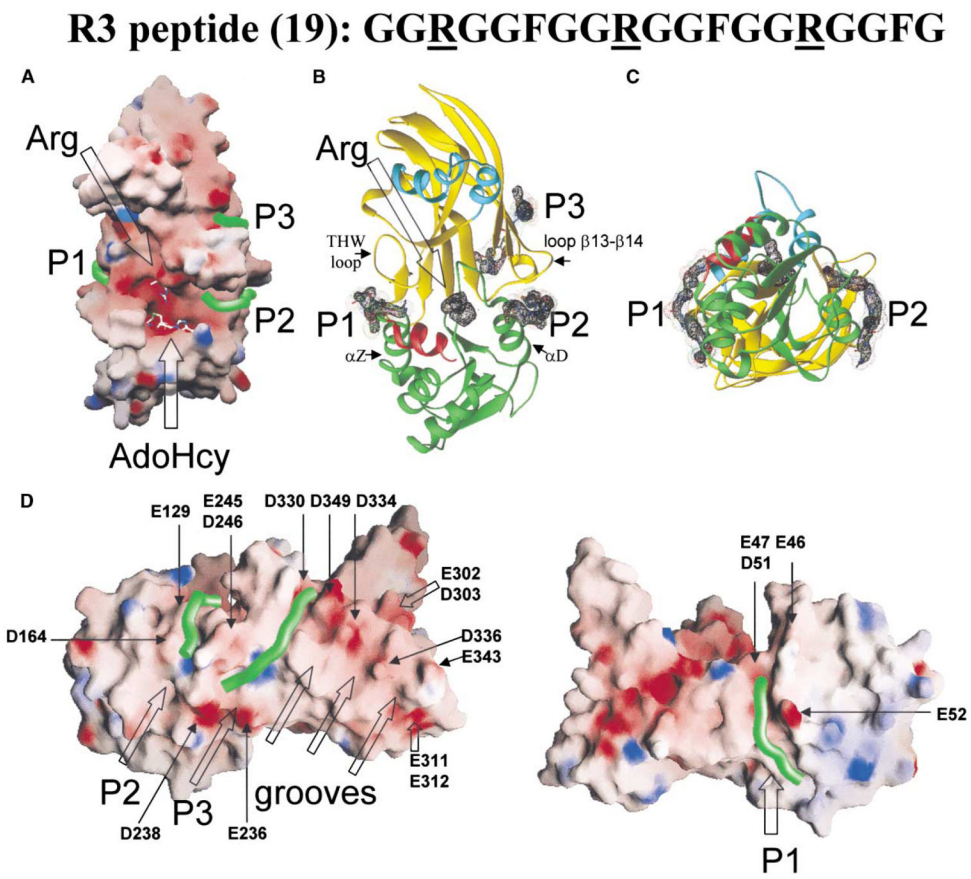

Figure 6. Structure of Ternary Complex of S14-AdoHcy-R3 Peptide (Sequence Shown at the Top)

(A) Solvent-accessible molecular surface with bound AdoHcy and Arg shown as stick models and indicated by the arrows. In the absence of helix αX (see Figure 3B), which is disordered in the PRMT1 crystals, AdoHcy is exposed and readily visible. The three discontinuous peptide binding sites P1, P2, and P3 are shown as green tubes.

(B) Ribbon representation of (A) with the three peptide binding sites shown as annealed omit electron densities (black) contoured at 5.0σ. Some of the structural elements flanking sites P2 and P3 are labeled.

(C) A 90° rotation of (B) showing that the binding sites P1 and P2 can be connected so that the middle Arg9 of peptide R3 is bound at the active site.

(D) Two side views of (A) showing the three peptide binding sites as well as other acidic grooves parallel to P3 (indicated by the arrows). The acidic residues flanking these grooves are labeled. In the left panel, it can be seen that connecting P2 and P3 would place the terminal arginine (Arg3 or Arg15) at one end of P2 in the active site.

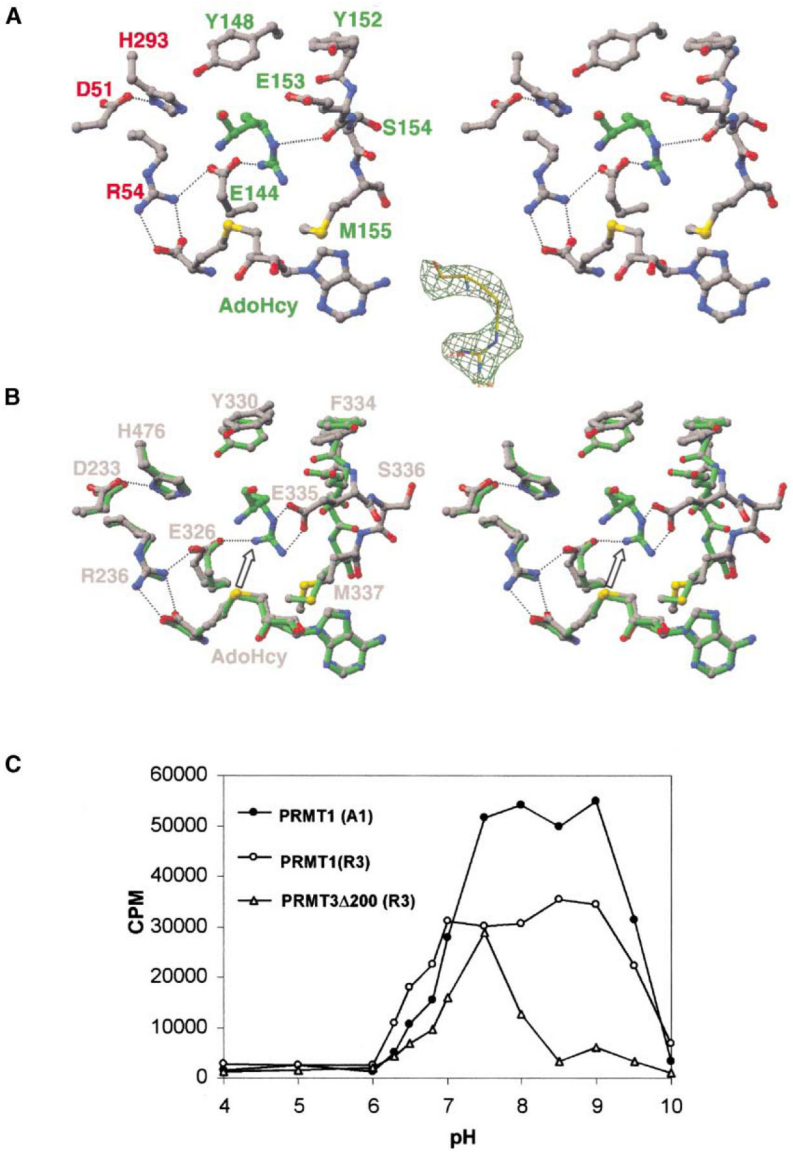

Figure 7. Active Sites of PRMT1 and PRMT3

(A) PRMT1 active site with bound Arg in stereo. The annealed omit electron density map, contoured at 5.0σ of the arginine, is shown as an insert.

(B) Superimposition of PRMT1 and PRMT3 (PDB ID code 1F3J) active sites in stereo. Only the PRMT3 residues are labeled. The arrow indicates transfer of the methyl group (attached to AdoHcy) to the bound Arg.

(C) pH dependence of PRMT1 and PRMT3 activities. Reactions (20 μl) contained 5 μM of purified hnRNP A1 or 100 μM of R3 peptide, 10 μg/ml of PRMT1 or 50 μg/ml of PRMT3Δ200, 40 μM [methyl-^{3}H]AdoMet (0.5 μCi) in 100 mM buffer, 200 mM NaCl, 2 mM EDTA, and 1 mM dithiothreitol. The buffers used were sodium acetate (pH 4 and 5), MES (pH 6.0, 6.3, 6.5, and 6.8), HEPES (pH 7.0 and 7.5), Tris (pH 8.0 and 8.5), and glycine (pH 9.0, 9.5, and 10.0). After incubating at 37°C for 15 min, 2.5 μl of 100 mg/ml BSA was added, followed by 0.5 ml of 20% TCA. The samples were filtered and washed three times

with 20% TCA through a GF/F filter (Millipore), dried, and subjected to liquid scintillation counting.

Table 1

Summary of Characterization of PRMT1 Mutants

					DLS size (kDa)		
Plasmid	**Protein**	**Expression**	**Solubility**	**GF Size (kDa)**	**−AdoHcy**	**+AdoHcy**	**Activity (hnRNP A1)**
pXC168	WT	++	+	320	780	440	100%
pXC246	WT (no tag)	+	+++	400	Not done	Not done	~100%
pXC247	M11 (no tag)	+++	+	250	360	330	~100%
pXC248	M11	+++	+	250	405	280	~100%
pXC249	S14	+	+++	250	>2 K	400	~100%
pXC250	S38	+++	+	250	240	240	Not detected
pXC256	L49	+++	−				
pXC252	E153Q	++	+	250	370	330	Not detected
pXC258	E153D	+++	+	300	450–3 K	320–400	~0.03%
pXC255	E144Q	+++	+	Void	>2 K	>2 K	~0.03%
pXC257	E144D	+++	+	600	970	620	10%
pXC335	M11 C254S	+++	+	250	Not done	375	~100%
pXC336	M11 ΔARM	+++	+/−	37	Not done	Not done	Not detected

The size of the oligomer is affected by the presence of cofactor AdoMet or product AdoHcy. In the absence of added AdoMet or AdoHcy, the protein eluted from gel filtration (GF) column S300HR (Pharmacia) as an asymmetrical peak with a long trailing tail, with the peak corresponding to a protein of about 500 kDa. When the protein was preincubated with AdoHcy, it eluted as a 320 kDa protein with a symmetrical elution profile. This is very similar to the endogenous PRMT1 in rat or HeLa cell extract, which eluted as a 330 kDa complex [8, 16]. Dynamic light scattering (DLS) measurement suggested that the size of PRMT1 oligomer is also influenced by temperature and protein concentration. The oligomer size has a lower limit of about 300 kDa but can go beyond 1000 kDa at lower temperature and higher protein concentration.

Table 2

Summary of X-Ray Data Collection and Model Refinement of PRMT1

Plasmid	**pXC248**	**pXC249**	**pXC252**
Protein complex	M11 + AdoHcy	S14 + AdoHcy + R3	E153Q + AdoHcy + R1
Cell dimensions (Å)	88.3 × 88.3 × 145.1	86.5 × 86.5 × 142.4	87.8 × 87.8 × 144.6
Resolution limit (Å)	2.50	2.35	2.64
Completeness (%)	98.6	96.3	99.8
R_{linear}	0.100	0.037	0.084
<I/σ(I)>	19.2	20.7	20.8
Observed reflections	102,483	77,491	116,340
Unique reflections	20,200	22,428	17,213
R_{value}	0.199	0.195	0.186
R_{free}	0.263	0.254	0.249
PDB	1ORI	IOR8	1ORH